Dysregulation of miR-34a Links Neuronal Development to Genetic Risk Factors for Bipolar Disorder

Sabine Bavamian[1,2,*], **Nikolaos Mellios**[3,*], **Jasmin Lalonde**[1,2,5,*], **Daniel M. Fass**[1,2], **Jennifer Wang**[1,2,4,6], **Steven D. Sheridan**[1,2,4,5,6], **Jon M. Madison**[1,2,4], **Fen Zhou**[1,2,4], **Erroll H. Rueckert**[1,2,4], **Doug Barker**[2], **Roy H. Perlis**[1,2,4,6], **Mriganka Sur**[3], and **Stephen J. Haggarty**[1,2,4,5,6]

[1]Chemical Neurobiology Laboratory, Center for Human Genetics Research, Massachusetts General Hospital, Boston, MA 02114 USA

[2]Stanley Center for Psychiatric Research, Broad Institute of MIT & Harvard, Cambridge, MA 02142 USA

[3]Department of Brain & Cognitive Sciences, Picower Institute for Learning & Memory, Massachusetts Institute of Technology, Cambridge, MA 02139 USA

[4]Department of Psychiatry, Massachusetts General Hospital, Harvard Medical School, Boston, MA 02114 USA

[5]Department of Neurology, Massachusetts General Hospital, Harvard Medical School, Boston, MA 02114 USA

[6]Center for Experimental Drugs & Diagnostics, Massachusetts General Hospital, Harvard Medical School, Boston, MA 02114 USA

Abstract

Bipolar disorder (BD) is a heritable neuropsychiatric disorder with largely unknown pathogenesis. Given their prominent role in brain function and disease, we hypothesized that microRNAs (miRNAs) might be of importance for BD. Here we show that levels of miR-34a, which is predicted to target multiple genes implicated as genetic risk factors for BD, are increased in postmortem cerebellar tissue from BD patients, as well as in BD patient-derived neuronal cultures generated by reprogramming of human fibroblasts into induced neurons (iNs) or into induced pluripotent stem cells (iPSCs) subsequently differentiated into neurons. Of the predicted miR-34a targets, we validated the BD risk genes ankyrin-3 (*ANK3*) and voltage-dependent L-type calcium channel subunit beta-3 (*CACNB3*) as direct miR-34a targets. Using human iPSC-derived neuronal progenitor cells (hNPCs), we further show that enhancement of miR-34a expression impairs neuronal differentiation, expression of synaptic proteins and neuronal morphology, whereas reducing endogenous miR-34a expression enhances dendritic elaboration. Taken together, we

Correspondence: Professor SJ Haggarty, 185 Cambridge Street, Boston, MA 02114, USA; shaggarty@mgh.harvard.edu.
*authors contributed equally to this work

Supplementary Information accompanies the paper on the Molecular Psychiatry website (http://www.nature.com/mp).

propose that miR-34a serves as a critical link between multiple etiological factors for BD and its pathogenesis through the regulation of a molecular network essential for neuronal development and synaptogenesis.

Keywords

miRNAs; miR-34a; bipolar disorder; iPSCs; stem cells; ANK3; CACNB3; neuronal differentiation

INTRODUCTION

Bipolar disorder (BD) is a genetically complex neuropsychiatric disorder affecting approximately 2–4% of the population that is characterized by recurrent episodes of depression and mania or hypomania[1, 2]. Although common- and rare-variant genetic association studies have begun to identify genes with variants conferring risk for developing BD, the pathogenesis of BD at a cellular level remains elusive. As a consequence, therapeutic options for BD are limited, consisting mainly of mood stabilizers developed decades ago, which are only effective in a subset of patients.

Recently, microRNAs (miRNAs), which are small, endogenous, non-coding RNAs (ncRNAs) of 18–23 nucleotides that post-transcriptionally regulate gene expression and are highly expressed in brain[3–7], have emerged as essential regulators of neuronal development, differentiation, and neuroplasticity[6, 8–11]. Understanding the function of miRNAs has led to the recognition of their ability to fine-tune the expression of numerous genes and orchestrate the overall activity of multiple pathway components, thereby positioning them to link numerous genetic risk factors for complex human genetic disorders into functional networks. An abundant literature now links miRNAs to neuropsychiatric disorders, especially through the analysis of the 22q11.2 schizophrenia susceptibility locus encompassing the miRNA processing gene *DGCR8*[12–15]. Moreover, alterations in miRNA profile have been identified in several psychiatric diagnoses including schizophrenia, autism, depression, addiction, and anxiety[6, 8, 10, 11, 16–18]. Indeed, recent evidence has shown that miR-137, a miRNA located within a locus that is associated with schizophrenia, may target a subset of important disease-related genes[19, 20], and potentially explain phenotypic heterogeneity[21, 22]. However, it remains unclear whether the SNPs in this region implicate miR-137 itself or an adjacent gene[23].

In the context of BD pharmacology, miR-34a, which belongs to the broadly evolutionarily conserved miR-34 microRNA family, has been shown to be reduced by lithium and valproic acid, two chemically distinct medications commonly used in the long-term treatment of BD[24, 25]. Moreover, miR-34a can influence mouse neuronal development[26] and its validated targets have been shown to be involved in neuronal differentiation, synaptic plasticity and long-term memory in mammals[27–29]. On the basis of these findings, we hypothesized that miR-34a could serve as an important link between emerging genetic risk factors for BD. Here, we show that miR-34a levels are increased in the cerebellum of BD subjects as well as in human neuronal cultures from reprogrammed patient cells. In addition, we provide evidence that miR-34a targets BD-related genes *ANK3* and *CACNB3*, and regulates their

expression during neuronal differentiation. Elevation of miR-34a expression in human iPSC-derived neuronal progenitors affected *ANK3* and *CACNB3* mRNA and protein expression and resulted in defects in neuronal differentiation as measured morphologically and biochemically through analysis of pre- and post-synaptic markers. Conversely, suppression of miR-34a expression enhanced dendritogenesis. Expanded profiling of the consequence of miR-34a overexpression revealed effects on a number of additional genes critical to neurodevelopment and implicated in the etiology of BD by recent human genetic studies[16, 30]. Taken together, our data highlight miR-34a as an important miRNA for BD and expand the knowledge on its effects on neuronal development.

MATERIALS AND METHODS

Postmortem human brain sample collection and RNA extraction

RNA samples (1–2 μg) from frontal cortex (BA9; 33 control and 31 BD samples), anterior cingulate cortex (29 control and 29 BD samples) and cerebellum (lateral cerebellar hemisphere; 34 control and 29 BD samples) were obtained from the Stanley Medical Research Institute (Chevy Chase, MD, USA) Array Collection. Quality and concentration of total RNA was measured using a NanoDrop ND-1000 spectrophometer (Thermo Fisher Scientific, Waltham, MA) and each sample was processed in triplicate for quantification of miR-34a and miR-34a target expression by quantitative real time PCR (qRT-PCR). miR-708 levels were measured in cerebellar samples only. The research met the criteria for Exemption 4 in terms of Human Subjects Research and was approved by the Institutional Review Board of the Massachusetts General Hospital.

Cell culture of proliferative human neural progenitors and differentiated neurons

Expandable human neuronal progenitor cells (hNPCs) from one unaffected male (GM08330, Coriell Institute for Medical Research) and one BD male (GM05224, Coriell Institute for Medical Research) were generated from iPSCs[31] (Madison *et al.*, manuscript under revision in Molecular Psychiatry) and cultured on poly-ornithine/laminin-coated six-well plates (BD Biosciences, San Jose, CA, USA) with neural expansion medium [70% Dulbecco's Modified Eagle Medium (DMEM) (Invitrogen, Carlsbad, CA, USA), 30% Ham's F-12 (Mediatech, Manassas, VA, USA) supplemented with B-27 (Invitrogen), 20 ng/ml each EGF (Sigma Sigma-Aldrich, St Louis, MO, USA) and bFGF (R&D Systems, Minneapolis, MN, USA)]. Terminal neural differentiation was achieved by plating NPCs at a seeding density of 4×10^4 cells per cm^2 on poly-ornithine/laminin-coated plates and culturing them for up to 8 weeks in differentiation medium [DMEM/F12 (Invitrogen), Glutamax (Invitrogen) supplemented with B-27 and N2 (Invitrogen), 200 μM L-ascorbic acid (Sigma) and 100 μM dibutryl-cAMP (Sigma)]. Culture medium was replaced every 3–4 days during neural differentiation. Cell samples were collected by manual scraping, pelleted by centrifugation to remove culture medium, quickly frozen on dry ice, and finally stored at –80°C.

Culture and transdifferentiation of human fibroblasts into induced neurons (iNs)

Human fibroblast lines were obtained from unrelated individuals age 18 and older recruited from an outpatient bipolar disorder clinic at Massachusetts General Hospital. Diagnosis of bipolar I disorder was confirmed by structured clinical interview (SCID-I)[32] conducted by a

board-certified psychiatrist, which was supplemented by referring clinician report and medical records where available. Structured clinical interview (SCID-I) was completed to exclude any Axis I disorder other than nicotine abuse or dependence. All subjects signed written informed consent prior to study participation. The study protocol was approved by the Institutional Review Board of the Massachusetts General Hospital.

Fibroblast cultures were grown on substrates coated with 0.1% gelatin (Millipore) in fibroblast media [DMEM (Invitrogen) containing 10% fetal bovine serum (FBS; Gemini Bio-products, Calabasas, CA, USA), non-essential amino acids, glutamate, and penicillin/streptomycin (Invitrogen)]. Lentiviral infection of human fibroblasts and conversion into induced neurons (iNs) were performed as described in[33] with minor modifications. Briefly, miR-9/9*-124 together with NEUROD2, ASCL1 and MYT1L (kindly provided by the Crabtree lab, Stanford University) were expressed in human fibroblasts. Infected cells were then maintained in fibroblast media supplemented with 1 mM valproic acid (VPA, Sigma) for 3–4 days before selection with appropriate antibiotics in Neuronal Medium (NM, ScienCell, Carlsbad, CA, USA) supplemented with 1 mM VPA for 7 days. 3–4 days after antibiotic selection, cells were passaged onto poly-ornithine/laminin (20 μg/mL) coated 96-well plates and maintained in NM supplemented with 1 mM VPA for an additional 7 days, after which VPA was withdrawn for the remaining differentiation period. Media were changed every 3–4 days. 38–40 days after the initial lentiviral transduction, cells were treated with RNA Protect Cell Reagent (Qiagen, Valencia, CA, USA). Then, RNA extraction was performed using miRNeasy Micro Kit (Qiagen) as per manufacturer's instructions.

miRNA and mRNA real-time quantitative RT-PCR

The miRNeasy Mini Kit (Qiagen) was used for RNA extraction per manufacturer's instructions. Quality and concentration of total RNA was assessed using a NanoDrop ND-1000 spectrophotometer (Thermo Fisher Scientific). For mature miRNA measurements, 10–20 ng of total RNA were reverse transcribed using Taqman microRNA reverse transcription kit (Life Technologies, Foster City, CA) and the product was diluted 1:15 in RNAse-free water. Levels of mature miRNAs, as well as normalizers RNU44 and U6 snRNAs, were assayed in triplicates following quantitative real time polymerase chain reaction with Taqman qRT-PCR assays (Life Technologies) and analyzed using the formula $C = 2^{Ct^{geomean\ of\ normalizers}} / 2^{Ct^{miRNA}}$. Both reverse transcription and qRT-PCR miRNA primers were part of Taqman miRNA assays (Life Technologies). miR-34a expression was normalized to U6 and RNU44 expression to control for the total amount of RNA present in each sample. For mRNA measurements, 300 ng of RNA were reverse transcribed using the VILO cDNA synthesis kit (Invitrogen). The geometric mean of β-actin and 18S rRNA or 18S rRNA alone was used for normalization using the following formula: $C = 2^{Ct^{normalizers}} / 2^{Ct^{mRNA}}$.

Bioinformatic prediction of miR-34a targets

To predict miR-34a targets, we used miRWalk database, http://www.umm.uni-heidelberg.de/apps/zmf/mirwalk/micrornapredictedtarget.html[34], which allows a comparative analysis by eight prediction programs (DIANAmT, miRanda, miRDB,

miRWalk, RNAhybrid, PICTAR, RNA22 and Targetscan)[35–41]. Our search was restricted to miRNA binding sites within the 3'UTR, with a minimum seed length of seven nucleotides between miR-34a sequence and its predicted targets. Due to performance differences between algorithms (i.e. sensitivity and specificity in target prediction), we retained only targets that were predicted by at least four different programs. We then compared this list to the BD GWAS list (140 genes published in[16]) and found 25 genes overlapping with both lists (see Table 1). For gene ontology analysis of miR-34a predicted targets, we used Targetscan 6.2 (http://www.targetscan.org/) and miR-34 family predicted targets were analyzed using DAVID Bioinformatics Resources 6.7 http://david.abcc.ncifcrf.gov/tools.jsp[42]. Gene ontology categories and disease enrichment were assayed (see Tables S3–S7).

Western blotting

For Western blot analyses, frozen cell pellets were rapidly re-suspended in ice-cold RIPA buffer (50 mM Tris-HCl [pH 8.0], 300 mM NaCl, 0.5% Igepal-630, 0.5% deoxycholic acid, 0.1% SDS, 1 mM EDTA) supplemented with protease inhibitors (Complete Protease Inhibitor without EDTA, Roche Applied Science, Indianapolis, IN) and phosphatase inhibitors (Phosphatase Inhibitor Cocktail A, Santa Cruz Biotechnology). One volume of 2× Laemmli buffer (100 mM Tris-HCl [pH 6.8], 4% SDS, 0.15% Bromophenol Blue, 20% glycerol, 200 mM β-mercaptoethanol) was added and the extracts were boiled for 5 min. Protein concentration for each sample was determined using the Pierce BCA Protein Assay Kit (Thermo Fisher Scientific, Rockford, IL, USA). Equal amount of lysate for each sample was separated using SDS-PAGE and transferred to a nitrocellulose membrane. After transfer, the membrane was blocked in TBST (Tris-buffered saline and 0.1% Tween 20) supplemented with 5% milk and probed with the indicated primary antibody at 4°C overnight. After washing with TBST, the membrane was incubated with the appropriate horseradish peroxidase (HRP)-conjugated secondary antibody (Santa Cruz Biotechnology, Santa Cruz, CA) and visualized using ECL reagents according to manufacturer guidelines (Pierce, Thermo Fisher Scientific). Quantification of each tested antigen was performed by densitometry analysis of three independent biological replicates.

Immunocytochemistry

Indirect immunofluorescence detection of antigens was carried out in hNPCs and differentiated neurons cultured on poly-ornithine/laminin-coated 96-well plates (Costar, Cambridge, MA) or similarly coated 24-well plates with glass coverslips. Cells were first washed twice with PBS and fixed for 30 minutes at room temperature with 4% PFA in PBS. After fixation, cells were washed twice with PBS, permeabilized with PBS-T (PBS and 0.25% Triton X-100) for 20 min, blocked in blocking solution (5% normal serum in PBS-T) for 30 min, and finally incubated overnight at 4°C with the first primary antibody in blocking solution. Next day, cells were washed with PBS and incubated for two hours at room temperature in the appropriate fluorophore-conjugated secondary antibody solution (Alexa 488- or 594-conjugated secondary antibody [Molecular Probes, Invitrogen] in blocking solution). After washes with PBS, cells were incubated again overnight in primary antibody solution for the second antigen and the procedure for conjugation of the fluorophore-conjugated secondary antibody was repeated as above. Finally, cell nuclei were

counterstained with 4',6-diamidino-2-phenylindole (DAPI) and washed twice before imaging using a fully automated epifluorescence microscope equipped with a 20× Fluor objective and a Photometrics CoolSNAP HQ 12-bits digital interline CCD camera (ImageXpress Micro, Molecular Devices, Sunnyvale, CA). For each condition, 4 wells were imaged with 6 different sites per well. Cells cultured on glass coverslips were mounted on glass slide with Prolong antifade reagent (Invitrogen) and imaged using a Zeiss Axio Observer Z1 inverted microscope.

Antibodies

The rabbit anti-ANK3 (Ankyrin-G; sc-28561), the goat anti-SOX1 (sc-17318) and the HRP-conjugated secondary antibodies were from Santa Cruz Biotechnology (Santa Cruz, CA). The chicken anti-GFP (A10262) and rat anti-mCherry (M11217) were from Life Technologies. The mouse anti-PSD95 (Clone K28/43, 75-028) was from NeuroMab, the rabbit anti-SOX2 (ab59776) from Abcam (Cambridge, MA), and the rabbit anti-Tuj1 (PRB-435P) from Covance (Richmond, CA). The rabbit anti-CACNB3 was purchased from LifeSpan BioSciences (Seattle, WA). The mouse monoclonals anti-Synaptophysin (S5768) and the anti-β-actin (A1978) were from Sigma. Finally, the rabbit anti-Musashi (AB5977) was from Millipore and the mouse anti-Synapsin 1 (106 001) as well as guinea pig anti-MAP2 (188 004) were purchased from Synaptic Systems (Gottingen, Germany).

Luciferase reporter constructs

The 3'UTRs of *CACNB3* (1116 bp, refseq. NM_000725.3), *DDN* (1698 bp, refseq. NM_015086.1) and *KLC2* (964 bp, refseq. NM_001134775.1) were PCR amplified from human brain cDNA (Invitrogen) and cloned downstream of the phosphoglycerate kinase I (PGK) promoter driven the luciferase reporter gene luc2 expression in the pmirGLO Dual-Luciferase miRNA Target Expression Vector (Promega, Madison, WI). The 3'UTR of *ANK3* (refseq. NM_001149.3), *CACNA1C* (refseq. NM_199460.2) and *SYT1* (refseq. NM_005639) were cloned by GeneCopoeia downstream of the SV40 promoter driven the secreted Gaussia luciferase (GLuc) reporter gene in a firefly/Renilla Duo-Luciferase reporter vector (pEZX-MT01). For miR-34a target validation, HEK293T cells were seeded at a density of 10^4 cells per well in a 96-well plate and grown for 24h before transient transfection with 20–40 ng of each dual luciferase reporter construct and 30 nM of pre-miR-34a or pre-miR-Neg (Ambion, Austin, TX) using Lipofectamine 2000 (Invitrogen). Luciferase activities were measured 48h after transfection using the Dual Glo Luciferase Assay System (#E2920, Promega) or the Luc-Pair miR Luciferase Assay Kit (LPFR-M030, GeneCopoeia) depending on the luciferase reporter constructs. Efficiency of transfection was normalized using Renilla luciferase activity.

Overexpression and suppression of miR-34a expression

For overexpression of miR-34a, hNPCs (unaffected male, derived from GM08330 iPSCs) were seeded at a density of 1.5×10^5 cells per well of a 12-well plate and transduced with the human Lenti-miR-34a or Lenti-miR-Ctrl expression system (Biosettia, San Diego, CA, USA) 2h after plating. The titer of the virus was ~1×10^7 infection units per mL and cells were transduced with a MOI = 33. Each miRNA precursor in the lentiviral vector was

cloned from its native context, including its flanking and stem-loop precursor sequence within the intron of human EF1α promoter region. This ensured that each miRNA was properly expressed and processed, and would function similarly to its endogenous form. miR-Ctrl has no DNA sequence inserted into the EF1α intron. A complete medium change was performed after 7h of transduction. Then, selection of NPCs expressing miR-34a or miR-Ctrl started after three days of transduction for 10 days with medium containing 1 μg/mL puromycin (Sigma). hNPCs stably expressing miR-34a and miR-Ctrl were expanded and seeded for subsequent differentiation.

For suppression of miR-34a expression, hNPCs (unaffected male, derived from GM08330 iPSCs) were transfected after 12 days of differentiation with either a construct expressing an anti-miR-34a sequence (GeneCopoeia, HmiR-AN0440-AM03-B) or a control scrambled sequence (GeneCopoeia, CmiR-AN0001-AM03). Since both constructs co-expressed mCherry as a reporter gene, for these experiments the 2 days transfected cells were fixed cells and immunostained for mCherry to allow complete visualization of the cells expressing the anti-miR constructs. The Sholl analysis was done as described above for the miR-34a overexpressing hNPCs. To assess the effect of the anti-miR-34a expression on target mRNAs, transfected cells were selected for 2 days using an antibiotic selection with hygromycin B at 200μg/ml.

Neuronal morphology measurement

For the analysis of the miR-Ctrl and miR-34a overexpressing hNPCs, the cells were seeded on glass coverslips at a density of 100,000 cells per well and differentiated as neurons. To measure the arbour complexity of the cells in both conditions after 3 weeks of differentiation, the cells were transfected at 19 days for 30 min with Lipofectamine 2000 and a plasmid encoding a membrane bound form of EGFP (Addgene, Plasmid 14757). 48h after transfection, the cells were then fixed and immunostained for GFP to enhance the signal and allow the complete visualization of the neuronal morphology. A total of 40 transfected neurons per condition from 5 biological replicates were captured using a Zeiss Axio Observer microscope and a 20× objective. The Sholl analysis was performed by superimposing concentric equidistant (10 μm) circles around the neuronal soma using Adobe Illustrator CS and counting the number of intersecting branches along the circumference of each circle. In a separate experiment, the effect of inhibiting miR-34a on the arbour complexity of differentiating hNPCs transfected with either the anti-miR-34a sequence (GeneCopoeia, HmiR-AN0440-AM03-B) or a control scrambled sequence (GeneCopoeia, CmiR-AN0001-AM03). Since both plasmids co-expressed mCherry as a reporter gene, for these experiments the fixed cells were then immunostained for mCherry to allow complete visualization of transfected cells, and Sholl analysis was done as described above for the miR-34a overexpressing hNPCs.

Multiplexed mRNA profiling assay using NanoString technology

Using a multiplexed, digital, mRNA profiling assay based upon NanoString single molecule, direct mRNA counting technology, we constructed a 131 unique gene probe set covering 18 genes located within the major loci identified to date through GWAS as being associated with BD susceptibility, as well as an additional 113 unique genes implicated in

neurodevelopment, functionally connected to ankyrin and ion channels, as well as in schizophrenia given the growing evidence for cross-disorder, shared genetic etiology by GWAS (Table S8)[23]. Data were normalized to the geometric mean of 13 selected reference genes (CBX3, DDX24, EEF1B2, NUDCD3, CEP170, NACAP1, LOC552889, ESD, MEA1, FAM162A, SEPT9, HP1BP3, RPRD1A) selected for flat expression signature in brain array data.

Data analysis and computational methods

Data are expressed as means ± standard error of mean (SEM). Statistical analysis was performed using GraphPad Prism6. Data distribution and normality was assayed using the Shapiro-Wilk or D'Agostino & Pearson omnibus normality tests. The Student two-tailed *t*-test (one sample or two-sample) or two-tailed Mann Whitney test was used for statistical comparison between two groups (based on normality) and ANOVA with Newman-Keuls Multiple Comparison Test was used for comparisons between more than two groups. Two-way ANOVA was used to estimate the effects of diagnosis and developmental stage in iPSC-generated neurons as well as quantify Western blot experiments. Post hoc comparisons between two means were conducted using the Bonferroni correction. The Spearman or Pearson correlation coefficients (based on normality) were applied for comparing correlations in post-mortem data in which one BD sample was excluded as outlier based on Grubb's test in miR-34a, two controls and one bipolar sample were excluded for very low normalizer expression for *ANK3* and *CACNB3* measurements. Student t-test for unpaired data with equal variance was applied for the Sholl analyses. In order to assess if there was evidence within the NanoString profiles for common molecular pathways being affected by miR-34a over expression, since the selection of 131 genes for inclusion in the NanoString probe set was purposely biased to cover genes implicated by neuropsychiatric genetics and ion channels, we deemed consideration of enrichment with Gene Ontology or related categories inappropriate. As an alternative computational approach to the systems-based modeling of the differential gene expression data, we determined if there were statistically significant properties of the protein-protein interaction network amongst the validated miR-34a target genes using VisANT 4.0 (http://visant.bu.edu) and/or the proteins encoded by the differentially expressed genes using DAPPLE v2.0 (Disease Association Protein-Protein Link Evaluator) (Figure 4).

RESULTS

miR-34a expression is increased in the cerebellum of BD patients and in cellular models derived from BD patients

Given the known influences of mood stabilizers on miR-34a levels and its potential role in neuronal maturation and plasticity, we decided to investigate the link between miR-34a and BD. Interestingly, two recent studies[43, 44], as well as unpublished data (S.J.H, manuscript in preparation), reported decreased expression of the two putative miR-34a targets *ANK3* and *CACNA1C* in cerebellum of BD individuals. Based on these findings and emerging literature linking the cerebellum with BD[43–52], we hypothesized that miR-34a could be dysregulated in the cerebellum of BD patients. To test this hypothesis, we measured miR-34a expression in postmortem human brain samples from cerebellum. We observed a significant increase in

miR-34a levels in the cerebellum of BD patients (N = 29) relative to healthy controls (N = 34) (Figure 1A), whereas no differences were seen in prefrontal cortex (PFC) or anterior cingulate cortex (Figure S1A and S1B). In contrast to this BD and brain region-specific difference in miR-34a expression, based on the recent identification by GWAS of a new susceptibility locus within the first intron of *ODZ4* where miR-708 is encoded[16], which is predicted to target both *ODZ4* itself and *CACNA1C*, the latter of which has shown multiple association with neuropsychiatric disorders[53], we also measured miR-708 in the same cerebellum samples from BD individuals (Figure S1C), but did not see any differences compared to the healthy controls. Therefore, we did not pursue the investigation of miR-708 targets and focused our study on miR-34a.

Since mood stabilizers have been shown to affect miR-34a expression[24, 25, 54], we segregated BD individuals based on whether or not they were under treatment with mood stabilizer medications (Figure 1B) and observed a significant increase in miR-34a expression only in BD individuals without treatment, suggesting a potential normalizing effect on miR-34a expression following treatment (Figure 1B). Interestingly, a significant correlation between age of onset of the disease and psychotic symptoms on miR-34a levels was observed (Figures S1D and S1E), without evidence for interaction of other confounding factors (Table S1, Figures S1F-H). Although sex differences did not significantly affect miR-34a levels in healthy control samples (data not shown), there was a more robust increase in miR-34a in female BD patients (Figure S1I).

Finally, to provide orthogonal validation of our findings in postmortem brain samples, and escape the known limitations of postmortem brain molecular analysis that until development of reprogramming technology has been the mainstay of functional analyses of molecular and cellular phenotypes in BD, we assessed the expression of miR-34a upon differentiation of human induced pluripotent stem cell (iPSC)-derived NPCs (hNPCs) generated from one BD patient (Madison *et al.*, manuscript under revision in Molecular Psychiatry) and their healthy parental (father) as a control[31]. The level of neuronal differentiation was evaluated by measuring multiple differentiation markers at different developmental stages (Figures 1C-D and S2A-F). Of note, both hNPC lines express the neural progenitor marker Nestin at similar level (Figure S2G). We found that miR-34a was expressed at low levels in hNPCs, and was modestly upregulated upon differentiation (Figure 1E). Unexpectedly, BD-derived hNPCs and neurons expressed significantly more miR-34a levels in comparison with the WT unaffected relative control samples. To complement these iPSC-based findings with a different, and a larger, set of control and patient-derived cellular models of BD, we turned to the use of newly developed, direct reprogramming methods to create induced neurons (iNs)[33]. As shown in Figure 1F, iNs were generated through the transdifferentiation of human fibroblasts derived from BD patients and psychiatrically-screened healthy controls. Similar to our findings comparing the healthy parental iPSC-derived neurons to those of the BD patient son, we found a significant increase in miR-34a expression in iNs derived from BD patients compared to healthy control cultures (Figure 1G). Taken together, these postmortem and cellular data, which have allowed the analysis of the molecular profiles of live human neurons generated using two different reprogramming approaches, suggest that miR-34a expression is dysregulated in the context of BD.

miR-34a targets BD risk genes *ANK3, CACNB3*, and *DDN*

Given the observed upregulation of miR-34a expression, we next aimed to identify miR-34a targets potentially relevant to the pathogenesis of BD through consideration of genetic risk factors recently identified by recent, large-scale, BD genome-wide association studies (GWAS) by the Psychiatric GWAS Consortium[16]. Using *in silico* analysis[34], we identified 25 overlapping miR-34a targets predicted by at least four different algorithms (Table 1).

Based on their known brain expression patterns and potential biological relevance in the context of neuropsychiatric disorders, we elected to follow up six of the 25 putative miR-34a targets that overlap with genes within the BD GWAS loci: *ANK3*, *CACNA1C*, *CACNB3*, *ODZ4*, *DDN*, and *KLC2*[16, 43, 44, 55, 56]. To further explore the putative miR-34a targets, we first checked the predicted binding site between the target mRNA and miR-34a using TargetScan (Table S2). Then, to experimentally validate the predicted miR-34a targets we needed to test whether the interaction sites between miR-34a and the mRNA targets are functional[57, 58]. Luciferase reporter assays revealed that miR-34a overexpression was capable of targeting and silencing the BD risk genes *ANK3*, *DDN*, and *CACNB3* along with the previously shown target gene *SYT1*[27], but had no effect on the 3'UTRs of *CACNA1C*, *ODZ4* and *KLC2* (Figure 2A). In addition, global analysis of miR-34a predicted targets showed enrichment of molecular networks related to neuronal development, differentiation and synaptic plasticity as well as gene sets implicated in neurodevelopmental disorders (Tables S3–S7[42]). Taken together, these results validate three genes implicated in BD risk as miR-34a targets and suggest that miR-34a may function to regulate an interacting molecular network important to BD pathogenesis through effects on neurodevelopment.

To further investigate the functional consequence of altering miR-34a expression throughout early neurodevelopment, we next assessed the expression of putative miR-34a targets upon differentiation of iPSC-derived NPCs (hNPCs). Among the six putative miR-34a targets, mRNA levels of four (*ANK3*, *CACNB3*, *ODZ4* and *KLC2*) were gradually increased until four weeks of differentiation, and then partially downregulated by eight weeks, whereas *CACNA1C* mRNA expression gradually increased during the eight weeks of differentiation (Figures 2B, 2C and Figure S3). *DDN* was not expressed in either hNPCs or differentiated neurons preventing its further analysis (data not shown). Since we observed an increase of miR-34a expression in BD patient-derived cellular models, we expected that expression of *bona fide* miR-34a targets would be decreased. Indeed, miR-34a validated targets were significantly downregulated in iPSC-derived neurons from BD individuals (Figures 2B-E).

As a further test of the correlation between miR-34a levels and its putative endogenous target genes in human iPSC-derived neurons, we used a miRNA inhibitor construct (anti-miR-34a) designed through its sequence complementarity to selectively trap endogenous miR-34a thereby preventing miR-34a association with its target genes along with a non-targeted control inhibitor construct (anti-scrambled). As a result of inhibiting endogenous miR-34a, expression of a miR-34a inhibitor construct is expected to reduce effects of miR-34a on mRNA stability and translational suppression resulting in an increase in target gene expression. The anti-miR-34a and anti-scrambled constructs were expressed in hNPCs from both the healthy control and BD son patient. After 2 weeks of differentiation, as shown

in Figure 2F, as predicted, expression of the anti-miR34a construct increased the expression of both ANK3 and CACNB3 in both the control and BD patient iPSC-derived neurons.

Finally, further emphasizing the reciprocally related expression of miR-34a and its putative targets, given the upregulation of miR-34a in the postmortem cerebellum of BD patients, we observed similarly decreased *ANK3* and *CACNB3* mRNA levels, which were also negatively correlated with miR-34a expression (Figures 2G-J). Of note, the limited amount of RNA collected from iNs did not allow further investigation of the correlation of targets to the level of miR-34a expression. Taken all together, these observations further support the validation of the two miR-34a targets *ANK3* and *CACNB3*.

miR-34a dysregulation alters differentiation of human iPSC-derived neurons

As a complement to the anti-miR-34a studies that showed an elevation of putative miR-34a target genes, to examine the effect of increasing miR-34a levels on target gene expression and neurodevelopment we stably overexpressed miR-34a in hNPCs from a healthy control subject and differentiated them for up to eight weeks (Figure 3A). miR-34a overexpression decreased levels of *ANK3* and *CACNB3* as observed in differentiated neurons relative to a negative control miRNA construct (miR-Ctrl) especially in the latest stages of differentiation (Figures 3B-E). Changes in target expression were not seen at the hNPC stage (Figures 3D-E), again pointing to a temporal dependency of the neurodevelopmental regulation of miR-34a targets. To further investigate how miR-34a upregulation observed in BD patient samples could affect pathophysiology, we assessed neuronal differentiation in miR-Ctrl and miR-34a overexpressing cells with a panel of biochemical markers (Figures 3D-E). Consistent with a blockade of neuronal differentiation, miR-34a overexpression delayed the expression of the presynaptic and postsynaptic neuronal markers SYP, SYN1 and PSD-95 over the neurodevelopmental time course (Figures 3D-E). In agreement with these findings, a similar phenotype was observed in 2 weeks differentiated neurons from the BD line in which miR-34a expression was previously found to be upregulated (Figure 3D). Of note, SYP and CACNB3 are not expressed at this stage of differentiation (Figure 3D). Moreover, ectopic overexpression of miR-34a and inhibition of endogenous miR-34a using an anti-miR-34a strategy altered neuronal morphology (Figures 3F-H) resulting in a significant reduction or increase of dendritic length and branch number when miR-34a expression was increased or decreased, respectively (Figures 3G-H). These results are highly reminiscent of those observed by Agostini *et al.*[26] in mouse cortical neurons revealing with this first demonstration in human neurons of an evolutionarily conserved function of miR-34a in the regulation of dendritic morphology.

Having demonstrated that manipulation of miR-34a expression in human iPSC-derived NPCs causes aberrant expression of synaptic proteins and the establishment of morphologically complex neurons, we sought next to determine the effects of miR-34a expression on a broader set of 18 genes implicated in neuropsychiatric disorders and neurodevelopment by recent GWAS of BD, as well as *SYP* and *SYN1* as controls based upon our Western blot data showing synaptic dysregulation (Figure 4, Figures S4–S6, Tables S8–S10 and Supplementary text). Using a multiplexed, digital, mRNA profiling assay based upon NanoString single molecule, direct mRNA counting technology, among the genes we

tested, miR-34a overexpression significantly affected the expression of 9 genes (*SYNE1, CACNA1C, CACNB3, SYN1, TNR, SYT12, SYP, ANK3, TMEM110*), with *ODZ4* and *ITIH4* close to having a significant difference (Figures 4A and S4).

To gain more insight into target genes either directly or indirectly affected by miR-34a overexpression over a temporally defined time course of human neurodevelopment, the miR-Ctrl and miR-34a overexpression lines were differentiated for 8 weeks with total RNA samples collected at t=0, 2, 4, 8 weeks in duplicate and subject to NanoString assay with a probe set consisting of a total of 131 genes, and the data merged with that from the t=6 weeks sets that were done in triplicates (Tables S8–S9). Using a cut off of a change greater than +/− 1.5-fold with miR-34a overexpression compared to the matched miR-Ctrl control, along with the requirement that at least two of the replicates showed concordant results for the particular time period, a total of 70 transcripts (53%) were identified at one more time point over the neurodevelopmental time course as showing differential expression (Table S10). Of these 70 transcripts, 14 were within one of the BD-associated GWAS loci, including both *ANK3* and *CACNB3*, which replicates with digital mRNA counting assay the qRT-PCR results and Western blot results shown in Figure 3. These 14 transcripts correspond to a frequency 78% of the 18 BD candidate genes assayed. Of the other non-BD candidate genes affected in the probe set, there were 56 genes corresponding to a frequency 49.6% of the total of the 113 non-BD candidate gene. Comparing these frequencies (77.8% BD genes vs. 49.6% non-BD genes) represents a statistically significant greater enrichment of affected BD candidate genes than that expected by chance ($p < 0.05$; two-tailed, Fisher's exact test) (Figure S5). In support of the notion that miR-34a targets a molecular network of interrelated proteins critical to neurodevelopment, analysis of protein-protein interactions amongst these newly validated (ANK3, CACNB3, DDN), previously validated (SYN1) targets and genes implicated by neuropsychiatric genetics[16, 19, 23] revealed a highly connected interaction network (Figures 4B and S6; See Supplemental text for details). Together, these findings support the hypothesis that elevation of miR-34a levels coordinately affects functionally connected pathways important for brain development and that dysregulation of miR-34a may be sufficient to affect the expression of multiple candidate BD susceptibility genes and genes critical to human neurodevelopment.

DISCUSSION

Despite the emerging knowledge on the importance of miRNAs in brain function and disease, very little is known about the role of miRNAs in BD. Here we show that miR-34a is upregulated in post-mortem BD brain and in two different patient-derived cellular models of BD, and is predicted to target multiple genes implicated in the etiology of BD through recent GWAS studies[16, 30]. In addition, we validate ANK3, CACNB3, and DDN as novel targets of miR-34a and implicate a molecular network of miR-34a targets. Lastly, we demonstrate using human iPSC-derived neuronal cultures that miR-34a expression is negatively correlated to that of ANK3 and CACNB3 and impairs neuronal differentiation and morphology. In this context, our finding that expression of an anti-miR-34a construct that traps endogenous miR-34a is sufficient to enhance dendritogenesis is particularly intriguing as it provides evidence that levels of one or more miR-34a target genes are rate-limiting for dendritic elaboration in human neurons.

While our study is the first to show that miR-34a inhibits neuronal differentiation of human neurons, previous studies in animal models have described the effects of miR-34a on neural stem cells[59], and neuronal progenitors[60], as well as on dendritic outgrowth and synaptic structure of neurons in culture[26]. Taken together with our results these studies suggest that although miR-34a inhibits neuronal maturation and synaptogenesis after the onset of neurogenesis, it is also capable of pushing neural stem cells to exit the cell cycle and become neuronal progenitors. Similar cell- and developmental stage- specific roles of miRNAs have before been described for other brain enriched miRNAs such as in the case of miR-134[61].

Among the novel validated miR-34a targets that we elucidated here, ANK3, is localized at the axon initial segment[62, 63], and recent findings have reported that it selectively decreased in the cerebellum of BD patients[44], the same brain region we observed to show elevated miR-34a levels in the present study. In addition, CACNB3 is involved in the regulation of surface expression and gating of the α-subunit (CACNA1C)[64], which has also been recently reported to be downregulated in the cerebellum of BD patients[43], (S.J.H., manuscript in preparation), and shown here to be indirectly affected my miR-34a overexpression as part of the NanoString profiling. Finally, in brain, DDN is a postsynaptic component of cytoskeletal modifications at the synapse that interacts with α-actinin and whose mRNA is localized to the synapse through a specific 3'UTR[65]. Therefore, the newly validated targets of miR-34a uncovered in our study are strongly linked to neuronal structure and function. Not surprisingly, when we analyzed miR-34a predicted targets for gene ontology parameters, we found that molecular networks related to neuronal development, differentiation and synaptic plasticity were among the top significant results (Tables S3–S6). In addition, the same *in silico* analysis revealed autism together with schizophrenia and depressive disorder among the top five diseases enriched in miR-34a predicted targets (Table S7). The validation of miR-34a targets through luciferase assays was supported by correlation data between miR-34a and its mRNA targets *ANK3* and *CACNB3*. Despite these negative correlations it is very likely that additional miRNAs or additional factors could be responsible for the changes in the levels of the targets during development[66]. It has also to be taken into account, though, that miRNAs and their targets are often in complex regulatory loops and the impact of miRNA-mediated inhibition can vary coherent and incoherent interactions[3, 67, 68], so that anti-correlated expression is not a prerequisite for miRNA targeting.

Chronic treatment with either lithium or valproic acid, which are the most effective mood-stabilizers, reduces miR-34a expression *in vivo* and in neuronal cultures[25]. On a similar note, chronic lithium and valproic acid co-treatment has been reported to downregulate miR-34a levels in rodent cerebellar granule cell cultures[24]. On the other hand, lithium treatment appears to have opposite effects in miR-34a expression in human peripheral blood-derived, lymphoblastoid cell lines[54]. More importantly, miR-34a has been shown in non-neuronal cells to be a strong inhibitor of WNT signalling and β-catenin-mediated transcription in response to p53 activation in non-neuronal cells[69, 70]. Recent findings have demonstrated that ANK3 regulates both cadherin and WNT signaling pathways by altering the availability of β-catenin with ANK3 loss-of-function impacting neurogenesis[71], supporting the importance of WNT signaling in the etiology of neurodevelopmental disorders. Given the

effects of lithium on WNT signalling, it is, therefore, intriguing to speculate that high miR-34a expression could be important for the pathophysiology of BD through this pathway, and that the delayed therapeutic effects of mood stabilizers could be partly attributed in their capacity to reduce miR-34a levels following chronic treatment.

We find our observation of selective dysregulation of miR-34a in the cerebellum consistent with growing evidence from the work of others and us demonstrating the selective dysregulation of genes implicated in BD etiology specifically in the cerebellum, namely ANK3 and CACNA1C, that have recently been reported[43, 44] (S.J.H., manuscript in preparation). While the PFC remains a brain region commonly implicated in BD pathophysiology, the potential importance of the cerebellum in BD and other affective disorders is increasingly apparent with recent neuroimaging studies having revealed complex connectivity with the cerebral cortex[45, 46, 51, 52, 72]. Given the well-known topographical organization of the cerebellum into specialized regions, including those critical to affective processing[72], future work in cerebellar subregions could help determine if miR-34a expression is dysregulated in areas implicated in control of emotional and affective behavior, and if these expression differences correlate with the selective dysregulated expression of *ANK3* and *CACNA1C* that has also been observed in the postmortem cerebellum samples[43, 44].

Though we did not see any differences in miR-34a expression in PFC nor ACC of BD patients compared to control individuals, we note that a recent study on the PFC from 15 BD patient samples and 15 non-psychiatric controls reported a modest 0.84-fold downregulation of miR-34a in PFC of BD patients relative to controls[73], and another study reported no difference[74]. Such discrepancies in gene expression between post-mortem brain cohorts may be due to disease heterogeneity and possible methodological reasons. Future studies with additional cohorts are needed to replicate our findings and to determine whether miR-34a alterations in BD are widespread in the brain or limited to specific brain regions as we observed. Addressing these questions will benefit from access to high-quality post-mortem brain tissue collections of sizes commensurate with the known phenotypic genetic heterogeneity of the disorder, along with sub-regional and ideally cell subtype specific. Being able to generate defined neuronal subtypes (e.g. cerebellar neurons) with authentic patterning of the human brain, will allow explicit test of the correlation between *in vitro* cellular models and post-mortem observations, the absence of which is a limitation of our current study.

While our studies employed a total of 8 (5 BD cases, 3 control) iNs and 2 (familial control and BD son) iPSCs, future studies with additional cohorts of well phenotyped BD patient and control fibroblasts reprogrammed into iNs and iPSCs are needed to determine whether miR-34a alterations in BD are common amongst all BD patients. These studies are likely to benefit from incorporation of a wider spectrum of neuropsychiatric disorder patients to understand how commonly variation in miR-34a is observed amongst patients with major depression, schizophrenia, and other disorders.

In summary, our study has implicated miR-34a as a small ncRNA dysregulated in BD that regulates multiple known BD-linked genes and can affect the *in vitro* differentiation of

human neurons. Further studies examining the regional expression and regulation of miR-34a-sensitive networks will provide critically needed insight into the pathogenesis of BD and may help elucidate new pathways for targeted therapeutic development.

Supplementary Material

Refer to Web version on PubMed Central for supplementary material.

REFERENCES

1. Ketter TA. Diagnostic features, prevalence, and impact of bipolar disorder. The Journal of clinical psychiatry. 2010; 71(6):e14. [PubMed: 20573324]

2. Craddock N, Sklar P. Genetics of bipolar disorder. Lancet. 2013; 381(9878):1654–1662. [PubMed: 23663951]

3. Bartel DP. MicroRNAs: target recognition and regulatory functions. Cell. 2009; 136(2):215–233. [PubMed: 19167326]

4. Krichevsky AM, King KS, Donahue CP, Khrapko K, Kosik KS. A microRNA array reveals extensive regulation of microRNAs during brain development. RNA. 2003; 9(10):1274–1281. [PubMed: 13130141]

5. Krol J, Loedige I, Filipowicz W. The widespread regulation of microRNA biogenesis, function and decay. Nature reviews Genetics. 2010; 11(9):597–610.

6. Mellios N, Sur M. The Emerging Role of microRNAs in Schizophrenia and Autism Spectrum Disorders. Frontiers in psychiatry. 2012; 3:39. [PubMed: 22539927]

7. Schratt G. microRNAs at the synapse. Nature reviews Neuroscience. 2009; 10(12):842–849. [PubMed: 19888283]

8. Green MJ, Cairns MJ, Wu J, Dragovic M, Jablensky A, Tooney PA, et al. Genome-wide supported variant MIR137 and severe negative symptoms predict membership of an impaired cognitive subtype of schizophrenia. Molecular psychiatry. 2013; 18(7):774–780. [PubMed: 22733126]

9. Miller BH, Wahlestedt C. MicroRNA dysregulation in psychiatric disease. Brain research. 2010; 1338:89–99. [PubMed: 20303342]

10. O'Connor RM, Dinan TG, Cryan JF. Little things on which happiness depends: microRNAs as novel therapeutic targets for the treatment of anxiety and depression. Molecular psychiatry. 2012; 17(4):359–376. [PubMed: 22182940]

11. Xu B, Karayiorgou M, Gogos JA. MicroRNAs in psychiatric and neurodevelopmental disorders. Brain research. 2010; 1338:78–88. [PubMed: 20388499]

12. Fenelon K, Mukai J, Xu B, Hsu PK, Drew LJ, Karayiorgou M, et al. Deficiency of Dgcr8, a gene disrupted by the 22q11.2 microdeletion, results in altered short-term plasticity in the prefrontal cortex. Proceedings of the National Academy of Sciences of the United States of America. 2011; 108(11):4447–4452. [PubMed: 21368174]

13. Fenelon K, Xu B, Lai CS, Mukai J, Markx S, Stark KL, et al. The pattern of cortical dysfunction in a mouse model of a schizophrenia-related microdeletion. The Journal of neuroscience : the official journal of the Society for Neuroscience. 2013; 33(37):14825–14839. [PubMed: 24027283]

14. Stark KL, Xu B, Bagchi A, Lai WS, Liu H, Hsu R, et al. Altered brain microRNA biogenesis contributes to phenotypic deficits in a 22q11-deletion mouse model. Nature genetics. 2008; 40(6): 751–760. [PubMed: 18469815]

15. Xu B, Hsu PK, Stark KL, Karayiorgou M, Gogos JA. Derepression of a neuronal inhibitor due to miRNA dysregulation in a schizophrenia-related microdeletion. Cell. 2013; 152(1–2):262–275. [PubMed: 23332760]

16. Large-scale genome-wide association analysis of bipolar disorder identifies a new susceptibility locus near ODZ4. Nature genetics. 2011; 43(10):977–983. [PubMed: 21926972]

17. Muinos-Gimeno M, Espinosa-Parrilla Y, Guidi M, Kagerbauer B, Sipila T, Maron E, et al. Human microRNAs miR-22, miR-138-2, miR-148a, and miR-488 are associated with panic disorder and regulate several anxiety candidate genes and related pathways. Biological psychiatry. 2011; 69(6): 526–533. [PubMed: 21168126]

18. Saba R, Schratt GM. MicroRNAs in neuronal development, function and dysfunction. Brain research. 2010; 1338:3–13. [PubMed: 20380818]

19. Genome-wide association study identifies five new schizophrenia loci. Nature genetics. 2011; 43(10):969–976. [PubMed: 21926974]

20. Kwon E, Wang W, Tsai LH. Validation of schizophrenia-associated genes CSMD1, C10orf26, CACNA1C and TCF4 as miR-137 targets. Molecular psychiatry. 2013; 18(1):11–12. [PubMed: 22182936]

21. Cummings E, Donohoe G, Hargreaves A, Moore S, Fahey C, Dinan TG, et al. Mood congruent psychotic symptoms and specific cognitive deficits in carriers of the novel schizophrenia risk variant at MIR-137. Neuroscience letters. 2013; 532:33–38. [PubMed: 22982201]

22. Lett TA, Chakavarty MM, Felsky D, Brandl EJ, Tiwari AK, Goncalves VF, et al. The genome-wide supported microRNA-137 variant predicts phenotypic heterogeneity within schizophrenia. Molecular psychiatry. 2013; 18(4):443–450. [PubMed: 23459466]

23. Ripke S, O'Dushlaine C, Chambert K, Moran JL, Kahler AK, Akterin S, et al. Genome-wide association analysis identifies 13 new risk loci for schizophrenia. Nature genetics. 2013; 45(10): 1150–1159. [PubMed: 23974872]

24. Hunsberger JG, Fessler EB, Chibane FL, Leng Y, Maric D, Elkahloun AG, et al. Mood stabilizer-regulated miRNAs in neuropsychiatric and neurodegenerative diseases: identifying associations and functions. American journal of translational research. 2013; 5(4):450–464. [PubMed: 23724168]

25. Zhou R, Yuan P, Wang Y, Hunsberger JG, Elkahloun A, Wei Y, et al. Evidence for selective microRNAs and their effectors as common long-term targets for the actions of mood stabilizers. Neuropsychopharmacology : official publication of the American College of Neuropsychopharmacology. 2009; 34(6):1395–1405. [PubMed: 18704095]

26. Agostini M, Tucci P, Steinert JR, Shalom-Feuerstein R, Rouleau M, Aberdam D, et al. microRNA-34a regulates neurite outgrowth, spinal morphology, and function. Proceedings of the National Academy of Sciences of the United States of America. 2011; 108(52):21099–21104. [PubMed: 22160706]

27. Agostini M, Tucci P, Killick R, Candi E, Sayan BS, Rivetti di Val Cervo P, et al. Neuronal differentiation by TAp73 is mediated by microRNA-34a regulation of synaptic protein targets. Proceedings of the National Academy of Sciences of the United States of America. 2011; 108(52): 21093–21098. [PubMed: 22160687]

28. Chi SW, Zang JB, Mele A, Darnell RB. Argonaute HITS-CLIP decodes microRNA-mRNA interaction maps. Nature. 2009; 460(7254):479–486. [PubMed: 19536157]

29. Wibrand K, Pai B, Siripornmongcolchai T, Bittins M, Berentsen B, Ofte ML, et al. MicroRNA regulation of the synaptic plasticity-related gene Arc. PloS one. 2012; 7(7):e41688. [PubMed: 22844515]

30. Muhleisen TW, Leber M, Schulze TG, Strohmaier J, Degenhardt F, Treutlein J, et al. Genome-wide association study reveals two new risk loci for bipolar disorder. Nature communications. 2014; 5:3339.

31. Sheridan SD, Theriault KM, Reis SA, Zhou F, Madison JM, Daheron L, et al. Epigenetic characterization of the FMR1 gene and aberrant neurodevelopment in human induced pluripotent stem cell models of fragile X syndrome. PloS one. 2011; 6(10):e26203. [PubMed: 22022567]

32. Spitzer RL, Williams JB, Gibbon M, First MB. The Structured Clinical Interview for DSM-III-R (SCID). I: History, rationale, and description. Archives of general psychiatry. 1992; 49(8):624–629. [PubMed: 1637252]

33. Yoo AS, Sun AX, Li L, Shcheglovitov A, Portmann T, Li Y, et al. MicroRNA-mediated conversion of human fibroblasts to neurons. Nature. 2011; 476(7359):228–231. [PubMed: 21753754]

34. Dweep H, Sticht C, Pandey P, Gretz N. miRWalk--database: prediction of possible miRNA binding sites by"walking" the genes of three genomes. Journal of biomedical informatics. 2011; 44(5):839–847. [PubMed: 21605702]

35. Griffiths-Jones S, Grocock RJ, van Dongen S, Bateman A, Enright AJ. miRBase: microRNA sequences, targets and gene nomenclature. Nucleic acids research. 2006; 34(Database issue):D140–D144. [PubMed: 16381832]

36. Krek A, Grun D, Poy MN, Wolf R, Rosenberg L, Epstein EJ, et al. Combinatorial microRNA target predictions. Nature genetics. 2005; 37(5):495–500. [PubMed: 15806104]

37. Lewis BP, Burge CB, Bartel DP. Conserved seed pairing, often flanked by adenosines, indicates that thousands of human genes are microRNA targets. Cell. 2005; 120(1):15–20. [PubMed: 15652477]

38. Maragkakis M, Reczko M, Simossis VA, Alexiou P, Papadopoulos GL, Dalamagas T, et al. DIANA-microT web server: elucidating microRNA functions through target prediction. Nucleic acids research. 2009; 37(Web Server issue):W273–W276. [PubMed: 19406924]

39. Miranda KC, Huynh T, Tay Y, Ang YS, Tam WL, Thomson AM, et al. A pattern-based method for the identification of MicroRNA binding sites and their corresponding heteroduplexes. Cell. 2006; 126(6):1203–1217. [PubMed: 16990141]

40. Rehmsmeier M, Steffen P, Hochsmann M, Giegerich R. Fast and effective prediction of microRNA/target duplexes. RNA. 2004; 10(10):1507–1517. [PubMed: 15383676]

41. Wang X. miRDB: a microRNA target prediction and functional annotation database with a wiki interface. RNA. 2008; 14(6):1012–1017. [PubMed: 18426918]

42. Huang da W, Sherman BT, Tan Q, Kir J, Liu D, Bryant D, et al. DAVID Bioinformatics Resources: expanded annotation database and novel algorithms to better extract biology from large gene lists. Nucleic acids research. 2007; 35(Web Server issue):W169–W175. [PubMed: 17576678]

43. Gershon ES, Grennan K, Busnello J, Badner JA, Ovsiew F, Memon S, et al. A rare mutation of CACNA1C in a patient with bipolar disorder, and decreased gene expression associated with a bipolar-associated common SNP of CACNA1C in brain. Molecular psychiatry. 2013

44. Rueckert EH, Barker D, Ruderfer D, Bergen SE, O'Dushlaine C, Luce CJ, et al. Cis-acting regulation of brain-specific ANK3 gene expression by a genetic variant associated with bipolar disorder. Molecular psychiatry. 2013; 18(8):922–929. [PubMed: 22850628]

45. Baldacara L, Nery-Fernandes F, Rocha M, Quarantini LC, Rocha GG, Guimaraes JL, et al. Is cerebellar volume related to bipolar disorder? Journal of affective disorders. 2011; 135(1–3):305–309. [PubMed: 21783257]

46. Buckner RL. The cerebellum and cognitive function: 25 years of insight from anatomy and neuroimaging. Neuron. 2013; 80(3):807–815. [PubMed: 24183029]

47. Eker C, Simsek F, Yilmazer EE, Kitis O, Cinar C, Eker OD, et al. Brain regions associated with risk and resistance for bipolar I disorder: a voxel-based MRI study of patients with bipolar disorder and their healthy siblings. Bipolar disorders. 2014

48. Kim D, Byul Cho H, Dager SR, Yurgelun-Todd DA, Yoon S, Lee JH, et al. Posterior cerebellar vermal deficits in bipolar disorder. Journal of affective disorders. 2013; 150(2):499–506. [PubMed: 23769608]

49. Liang MJ, Zhou Q, Yang KR, Yang XL, Fang J, Chen WL, et al. Identify changes of brain regional homogeneity in bipolar disorder and unipolar depression using resting-state FMRI. PloS one. 2013; 8(12):e79999. [PubMed: 24324588]

50. Smolin B, Karry R, Gal-Ben-Ari S, Ben-Shachar D. Differential expression of genes encoding neuronal ion-channel subunits in major depression, bipolar disorder and schizophrenia:

implications for pathophysiology. Int J Neuropsychopharmacol. 2012; 15(7):869–882. [PubMed: 22008100]

51. Soontornniyomkij B, Everall IP, Chana G, Tsuang MT, Achim CL, Soontornniyomkij V. Tyrosine kinase B protein expression is reduced in the cerebellum of patients with bipolar disorder. Journal of affective disorders. 2011; 133(3):646–654. [PubMed: 21612826]

52. Villanueva R. The cerebellum and neuropsychiatric disorders. Psychiatry research. 2012; 198(3): 527–532. [PubMed: 22436353]

53. Identification of risk loci with shared effects on five major psychiatric disorders: a genome-wide analysis. Lancet. 2013; 381(9875):1371–1379. [PubMed: 23453885]

54. Chen H, Wang N, Burmeister M, McInnis MG. MicroRNA expression changes in lymphoblastoid cell lines in response to lithium treatment. Int J Neuropsychopharmacol. 2009; 12(7):975–981. [PubMed: 19254429]

55. Du J, Wei Y, Liu L, Wang Y, Khairova R, Blumenthal R, et al. A kinesin signaling complex mediates the ability of GSK-3beta to affect mood-associated behaviors. Proceedings of the National Academy of Sciences of the United States of America. 2010; 107(25):11573–11578. [PubMed: 20534517]

56. Ferrandiz-Huertas C, Gil-Minguez M, Lujan R. Regional expression and subcellular localization of the voltage-gated calcium channel beta subunits in the developing mouse brain. Journal of neurochemistry. 2012; 122(6):1095–1107. [PubMed: 22737983]

57. Huang Y, Zou Q, Song H, Song F, Wang L, Zhang G, et al. A study of miRNAs targets prediction and experimental validation. Protein & cell. 2010; 1(11):979–986. [PubMed: 21153515]

58. Kuhn DE, Martin MM, Feldman DS, Terry AV Jr, Nuovo GJ, Elton TS. Experimental validation of miRNA targets. Methods. 2008; 44(1):47–54. [PubMed: 18158132]

59. Aranha MM, Santos DM, Sola S, Steer CJ, Rodrigues CM. miR-34a regulates mouse neural stem cell differentiation. PloS one. 2011; 6(8):e21396. [PubMed: 21857907]

60. Fineberg SK, Datta P, Stein CS, Davidson BL. MiR-34a represses Numbl in murine neural progenitor cells and antagonizes neuronal differentiation. PloS one. 2012; 7(6):e38562. [PubMed: 22701667]

61. Gaughwin P, Ciesla M, Yang H, Lim B, Brundin P. Stage-specific modulation of cortical neuronal development by Mmu-miR-134. Cereb Cortex. 2011; 21(8):1857–1869. [PubMed: 21228099]

62. Clark BA, Monsivais P, Branco T, London M, Hausser M. The site of action potential initiation in cerebellar Purkinje neurons. Nature neuroscience. 2005; 8(2):137–139. [PubMed: 15665877]

63. Komada M, Soriano P. [Beta]IV-spectrin regulates sodium channel clustering through ankyrin-G at axon initial segments and nodes of Ranvier. The Journal of cell biology. 2002; 156(2):337–348. [PubMed: 11807096]

64. Yamaguchi H, Hara M, Strobeck M, Fukasawa K, Schwartz A, Varadi G. Multiple modulation pathways of calcium channel activity by a beta subunit. Direct evidence of beta subunit participation in membrane trafficking of the alpha1C subunit. The Journal of biological chemistry. 1998; 273(30):19348–19356. [PubMed: 9668125]

65. Kremerskothen J, Kindler S, Finger I, Veltel S, Barnekow A. Postsynaptic recruitment of Dendrin depends on both dendritic mRNA transport and synaptic anchoring. Journal of neurochemistry. 2006; 96(6):1659–1666. [PubMed: 16464232]

66. Mellios N, Huang HS, Grigorenko A, Rogaev E, Akbarian S. A set of differentially expressed miRNAs, including miR-30a-5p, act as post-transcriptional inhibitors of BDNF in prefrontal cortex. Human molecular genetics. 2008; 17(19):3030–3042. [PubMed: 18632683]

67. Liu H, Kohane IS. Tissue and process specific microRNA-mRNA co-expression in mammalian development and malignancy. PloS one. 2009; 4(5):e5436. [PubMed: 19415117]

68. Osella M, Bosia C, Cora D, Caselle M. The role of incoherent microRNA-mediated feedforward loops in noise buffering. PLoS computational biology. 2011; 7(3):e1001101. [PubMed: 21423718]

69. Hashimi ST, Fulcher JA, Chang MH, Gov L, Wang S, Lee B. MicroRNA profiling identifies miR-34a and miR-21 and their target genes JAG1 and WNT1 in the coordinate regulation of dendritic cell differentiation. Blood. 2009; 114(2):404–414. [PubMed: 19398721]

70. Kim NH, Kim HS, Kim NG, Lee I, Choi HS, Li XY, et al. p53 and microRNA-34 are suppressors of canonical Wnt signaling. Science signaling. 2011; 4(197):ra71. [PubMed: 22045851]

71. Durak O, de Anda FC, Singh KK, Leussis MP, Petryshen TL, Sklar P, et al. Ankyrin-G regulates neurogenesis and Wnt signaling by altering the subcellular localization of beta-catenin. Molecular psychiatry. 2014

72. Stoodley CJ, Schmahmann JD. Evidence for topographic organization in the cerebellum of motor control versus cognitive and affective processing. Cortex; a journal devoted to the study of the nervous system and behavior. 2010; 46(7):831–844.

73. Smalheiser NR, Lugli G, Zhang H, Rizavi H, Cook EH, Dwivedi Y. Expression of microRNAs and Other Small RNAs in Prefrontal Cortex in Schizophrenia, Bipolar Disorder and Depressed Subjects. PloS one. 2014; 9(1):e86469. [PubMed: 24475125]

74. Kim AH, Reimers M, Maher B, Williamson V, McMichael O, McClay JL, et al. MicroRNA expression profiling in the prefrontal cortex of individuals affected with schizophrenia and bipolar disorders. Schizophrenia research. 2010; 124(1–3):183–191. [PubMed: 20675101]
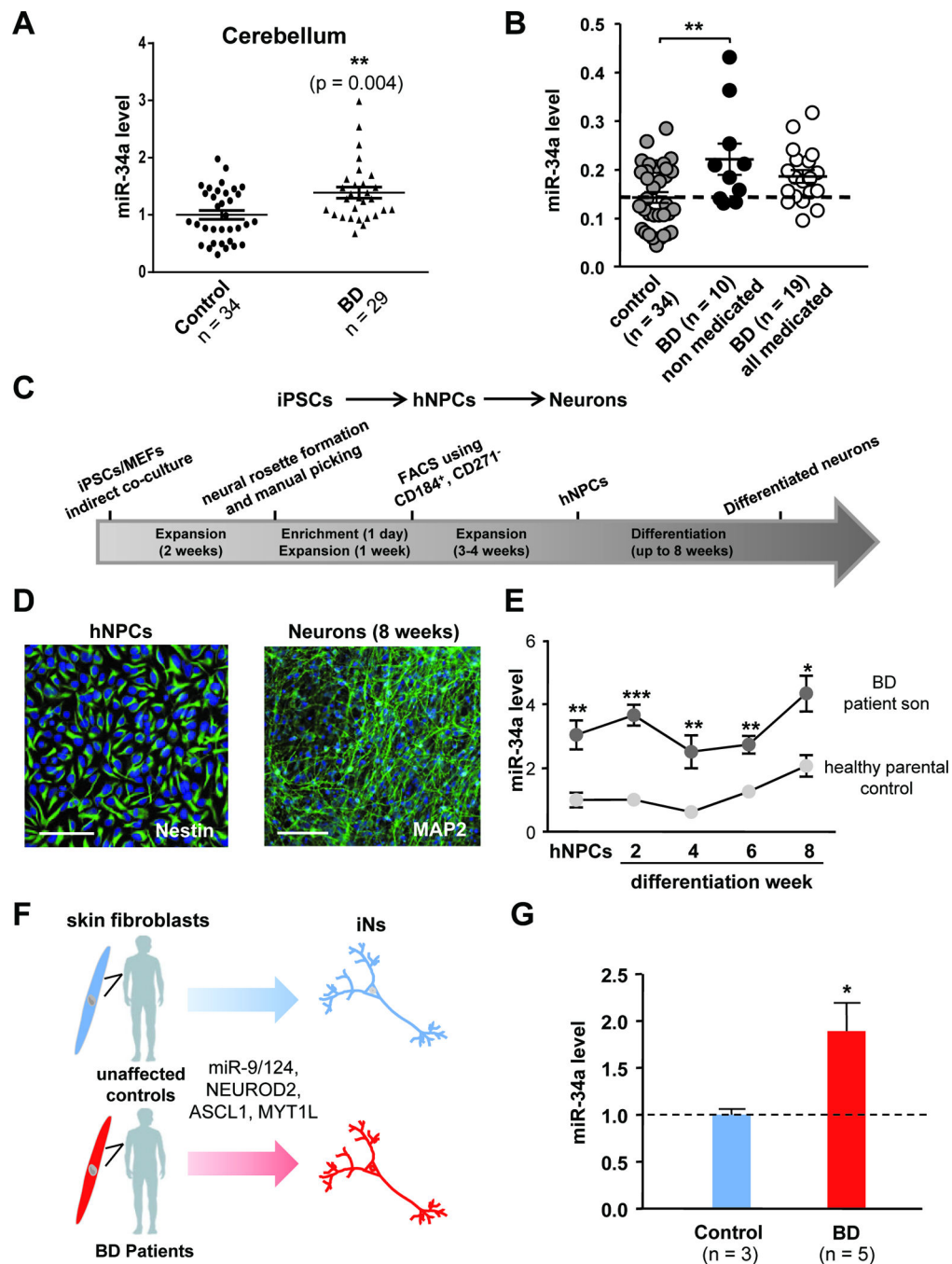
Figure 1. miR-34a expression is increased in the cerebellum of BD patients and in patient-derived cellular models of BD

A) Mean ± SEM miR-34a levels depicted as fold change relative to controls. N = 34 control and 29 BD cerebellar samples. **p<0.01 compared to control conditions, based on a two-tailed, one-sample *t*-test. B) Mean ± SEM miR-34a levels in cerebellum of controls (N = 34) and BD patients segregated into medicated (N = 19) and non-medicated (N = 10). **p<0.01 based on ANOVA with Tukey's Multiple Comparison Test. C) Schematic of the neuronal differentiation process from iPSCs to eight weeks differentiated neurons. D) Immunostaining of Nestin in hNPCs and MAP2 in eight weeks differentiated neurons, scale

bar = 50 μm. E) Graphs showing relative miR-34a expression in hNPCs and differentiated neurons of a healthy control individual (light grey circles) and a BD patient (dark grey circles). Data are shown as fold change relative to miR-34a level at hNPC stage. Stars over data depict statistical significance based on a two-tailed *t*-test (*p<0.05, **p<0.01, *p<0.001). F) Schematic of induced neurons (iNs) generation. G) miR-34a expression in iNs from three control and five BD subjects. The graph shows mean ± SEM miR-34a expression relative to control iNs. miR-34a expression was normalized to U6 and RNU44 expression, which control for the total amount of RNA present in each sample. *p<0.05 compared to control conditions, based on a two-tailed, one-sample *t*-test.
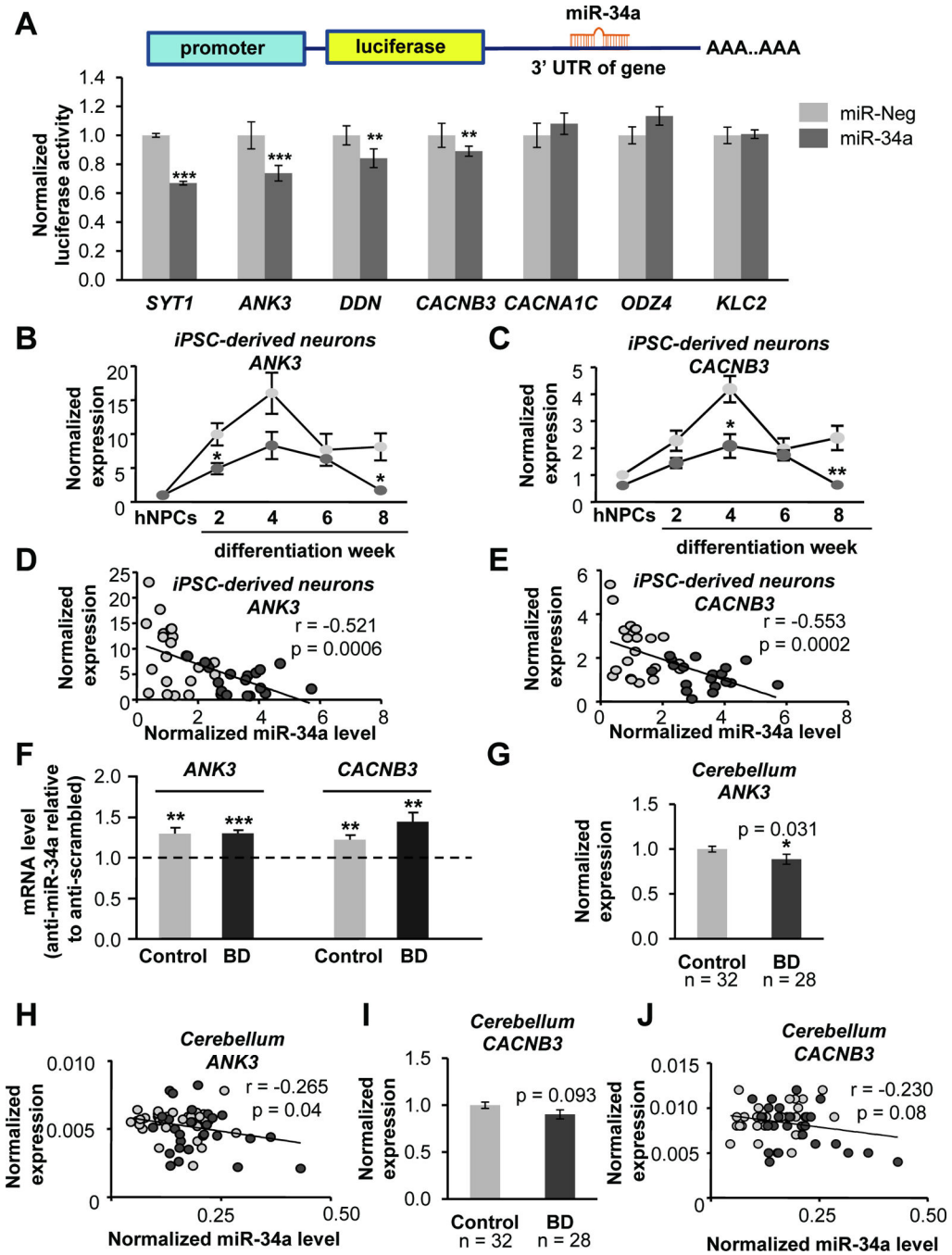
Figure 2. Bipolar disorder-related genes differentially expressed during differentiation of human iPSC-derived neuronal progenitors are targets of miR-34a

A) Upper: Schematic of luciferase assay. The interaction of a putative target with miR-34a is shown. Lower: Results from luciferase reporter gene assays in HEK293T transfected with either a non-targeting control having no sequence homology to the human (miR-Neg - light grey bars) or miR-34a mimics (dark grey bars). Data are shown as fold change relative to miR-Neg treatment. **p<0.01, ***p<0.001 compared to miR-Neg treatment, based on a two-tailed, one-sample *t*-test. B-E) Expression (B-C) and correlation (D-E) data relative to

miR-34a expression of the two validated miR-34a targets *ANK3* (B, D) and *CACNB3* (C, E) in control (light grey bars) and BD (dark grey bars) iPSC-derived NPCs/neurons. Data are shown as fold change relative to miR-34a level at hNPC stage. Stars over data depict statistical significance based on a two-tailed *t*-test (*p<0.05, **p<0.01, ***p<0.001). Spearman correlation coefficients (r) and p values (two-tailed) are shown. F) Control (light grey bars) and BD patient (dark grey bars) iPSC-derived NPCs were transfected with either an anti-miR-scrambled or anti-miR-34a construct designed to trap endogenous miR-34a and differentiated for two weeks. Data show expression of the two validated miR-34a targets *ANK3* and *CACNB3* expressed as the ratio of anti-miR34a to anti-miR-scrambled. Stars over data depict statistical significance based on a two-tailed *t*-test (**p<0.01, ***p<0.001). G-J) Expression (G-I) and correlation (H-J) data relative to miR-34a expression of *ANK3* (G, H) and *CACNB3* (I, J) in the cerebellum of controls (light grey bar, N = 32) and BD patients (dark grey bar, N = 28). Star and p-value depicted in (G) and (I) are based on two-tailed, Mann-Whitney test (*p<0.05). Pearson correlation coefficients (r) and p values (two-tailed) are shown.
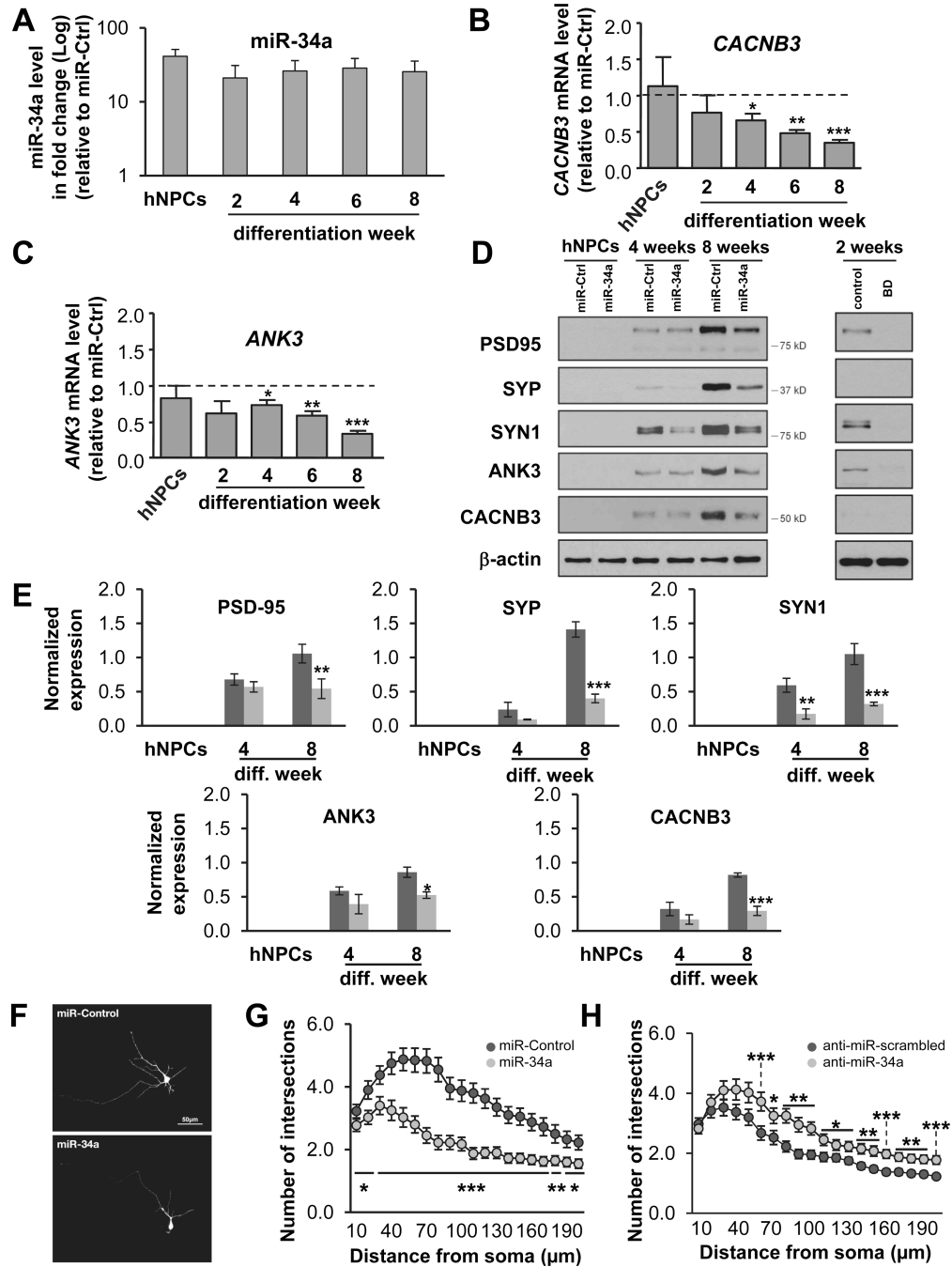
Figure 3. Ectopic expression of miR-34a decreases CACNB3 and ANK3 expression and affects neuronal differentiation and morphology of human iPSC-derived neurons

A) hNPCs were transduced with either miR-Ctrl or miR-34a lentiviral constructs and differentiated for eight weeks. Data show expression of miR-34a shown as fold change relative to the transcript level at the initial hNPC stage. B-C) Follow-up of the two validated miR-34a targets *ANK3* and *CACNB3* at transcriptional level in miR-Ctrl and miR-34a overexpressing hNPCs and differentiated neurons. Data are shown as fold change relative to the transcript of interest at hNPC stage and normalized to the transcript level in miR-Ctrl conditions. Data are mean ± SEM from three independent experiments. *p <0.05, **p<0.01,

***p<0.001 compared to miR-Ctrl treatment, based on a two-tailed, one-sample *t*-test. D) PSD95, Synaptophysin (SYP), Synapsin-1 (SYN1), ANK3 and CACNB3 Western blot results on hNPCs, four and eight weeks differentiated neurons overexpressing either miR-Ctrl or miR-34a (left panel) or two weeks differentiated control and BD neurons (right panel). β-actin was used as internal standard. E) Quantification of Western blot data in (D) by densitometric analysis. The bars show the mean ± SEM ratio of the protein of interest and β-actin signals, as evaluated by densitometric analysis of three independent biological replicates. *p <0.05, **p<0.01, ***p<0.001 compared to miR-Ctrl treatment, based on a two-way ANOVA using the Bonferroni correction as *post hoc* comparisons between two means. F) Image-based analysis of the effect of miR-34a overexpression on the morphology of hNPCs after three weeks of differentiation with sparse transfection with membrane-targeted GFP for two days, scale bar = 50 μm. G-H) Graph showing the number of branches in function of the soma distance in (G), three weeks differentiated neurons overexpressing miR-Ctrl (dark grey circles) and miR-34a (light grey circles) or in (H), two weeks differentiated neurons expressing anti-miR-scrambled control (dark grey circles) and anti-miR-34a (light grey circles). 12 days differentiated cells were transfected with anti-miR constructs for 2 days. Since both constructs co-expressed mCherry as a reporter gene, cells expressing the anti-miR constructs were immunostained for mCherry. For each condition, a total of 40 neurons were imaged and quantified using classical Sholl analysis. *p <0.05, **p<0.01, ***p<0.001 compared to miR-Ctrl treatment (G) or anti-miR-scrambled (H), based on a two-tailed *t*-test.
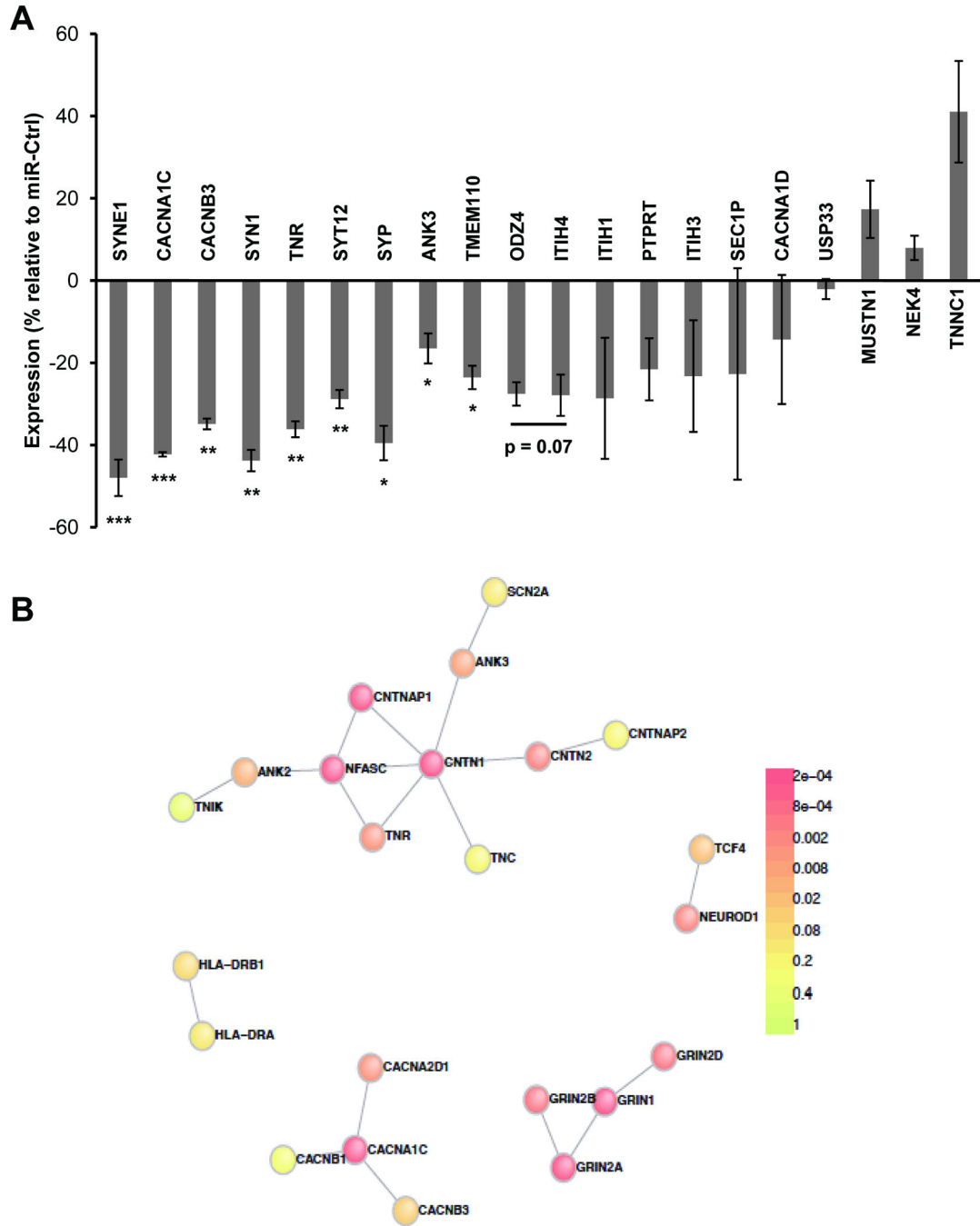
Figure 4. miR-34a overexpression affects BD-risk genes that are highly connected through a protein interaction network

A) Data show expression of 18 BD-risk genes (*SYNE1*, *CACNA1C*, *CACNB3*, *TNR*, *SYT12*, *ANK3*, *TMEM110*, *ODZ4*, *ITIH4*, *ITIH1*, *PTPRT*, *ITIH3*, *SEC1P*, *CACNA1D*, *USP33*, *MUSTN1*, *NEK4* and *TNCC1*) and two validated miR-34a targets (*SYN1* and *SYT*) measured in six week differentiated neurons overexpressing either miR-Ctrl or miR-34a. Data are expressed in percentage relative to miR-Ctrl overexpressing neurons with n=3 replicates. *p<0.05, **p<0.01, ***p<0.001 compared to miR-Ctrl treatment based on a two-tailed, one-

sample *t*-test. B) Direct protein-protein interactions amongst genes differentially affected by miR-34a overexpression over a neurodevelopmental time course (t=0, 2, 4, 8 weeks in duplicate; t=6 weeks in triplicate) in human iPSC-derived NPCs visualized using DAPPLE v2.0. Color coding corresponds to p-value from 5,000 within-degree, node-label permutations. See Supplemental Text for additional details.

Table 1

List of the 25 predicted miR-34a targets overlapping with BD GWAS and with a score > 4

List of predicted miR-34a targets was generated using miRWalk database that considers eight different target prediction programs. Only targets ... code: green = pr...

b

a

#	Gene	DIANAmT	miRanda	miRDB	miRWalk	RNAhybrid	PICTAR	RNA22	Targetscan	SUM
1	ANK3	1	1	1	1	1	1	1	1	8
2	CACNB3	1	1	1	1	1	0	1	1	7
3	PACS1	1	1	1	1	1	0	1	1	7
4	DPP3	1	1	1	1	1	0	0	1	6
5	LMBR1L	1	1	0	1	0	1	1	1	6
6	SPTBN2	1	1	0	1	1	1	0	1	6
7	KLC2	1	1	0	1	0	0	1	1	5
8	C2orf55	1	1	0	1	1	0	0	1	5
9	FUT1	1	1	1	1	0	0	0	1	5
10	LBA1	1	1	0	1	0	1	0	1	5
11	MGAT4A	1	1	1	1	0	0	0	1	5
12	RAB1B	1	1	0	1	0	1	0	1	5
13	SH3PXD2A	1	1	1	1	0	0	0	1	5
14	CACNA1C	1	1	0	1	0	0	0	1	4
15	BBS1	1	1	0	1	0	0	0	1	4
16	CNNM4	1	1	0	1	0	0	0	1	4
17	DDN	1	1	0	1	0	0	0	1	4
18	LMAN2L	1	0	0	1	1	0	0	1	4
19	MRPL30	1	1	0	1	0	0	0	1	4
20	ODZ4	1	1	0	1	0	0	0	1	4
21	PPM1M	1	0	0	1	0	1	0	1	4
22	PRKAG1	1	1	0	1	0	0	0	1	4
23	RIN1	1	1	0	1	0	0	0	1	4
24	SEMA3G	1	1	0	0	0	1	0	1	4
25	ZMIZ1	1	1	0	1	0	0	0	1	4